Results in Engineering 25 (2025) 104577

Contents lists available at ScienceDirect

Results in Engineering

journal homepage: www.sciencedirect.com/journal/results-in-engineering

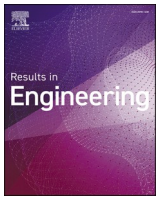

Numerical simulation of hotspot in polyol ester production using microwave-assisted reaction

Nur Atiqah Mohamad Aziz [a,b,*], Hassan Mohamed [a,c], Mei Yin Ong [a], Robiah Yunus [d], Ming Chiat Law [e], Hamidah Abd Hamid [a], Dina Kania [f], Teuku Meurah Indra Mahlia [g]

[a] Institute of Sustainable Energy, Universiti Tenaga Nasional, Putrajaya Campus, Jalan IKRAM-UNITEN, 43000, Kajang, Selangor, Malaysia
[b] Department of Chemical and Process Engineering, Faculty of Engineering and Built Environment, Universiti Kebangsaan Malaysia, UKM Bangi, 43600, Selangor, Malaysia
[c] Mechanical Engineering Department, College of Engineering, Universiti Tenaga Nasional, Putrajaya Campus, Jalan IKRAM-UNITEN, 43000, Kajang, Selangor, Malaysia
[d] Department of Chemical and Environmental Engineering, Universiti Putra Malaysia, Serdang, 43400, Selangor, Malaysia
[e] Mechanical Engineering Department, Curtin University Malaysia, CDT 250, 98009, Miri, Sarawak, Malaysia
[f] Department of Petroleum Engineering, Faculty of Engineering, Universitas Islam Riau, Pekanbaru, Indonesia
[g] Centre for Technology in Water and Wastewater, School of Civil and Environmental Engineering, Faculty of Engineering and Information Technology, University of Technology Sydney, NSW, 2007, Australia

ARTICLE INFO

Keywords:
Green energy
Hotspot
Microwave heating
Polyol ester
Transesterification

ABSTRACT

The complex distribution of electric field and heat transfer in microwave heating causes unfavorable hotspots in a microwave-assisted transesterification process. This local overheating may reduce product yield significantly, thereby highlighting the importance of mixing during microwave-assisted biolubricant production. This study investigated the distribution of electric field in the microwave-assisted transesterification of palm oil methyl ester (PME) and trimethylolpropane (TMP) for biolubricant trimethylolpropane ester (TMPE) production, as well as the temperature profile and the power absorbed, using COMSOL Multiphysics 4.2. The electric field and power absorbed by the sample were 1.92×10^4 V/m and 1.38×10^7 W/m^3, respectively, which are highly affected by the polarity of TMPE. Hotspots were observed and were primarily located in the upper corner of the TMPE sample, and a significant redistribution of the electromagnetic field within the oven cavity was measured. This study also concluded that the dielectric properties of the TMPE sample layer and frequency are highly influential factors for microwave absorption and heat conversion. This study can provide insight into the future design of microwave-assisted transesterification to enhance product yield and scale up microwave reactors.

1. Introduction

Microwave radiation is an excellent technique for accelerating transesterification reactions due to its rapid and volumetric heating mechanism. Unlike conventional heating, in which heat is transferred through thermal conduction and convection over the wall before reaching the target medium, microwave heating allows the direct heating of the sample through dipolar polarization and ionic conduction, bypassing the need to heat the surrounding walls [1]. Hence, heat transfer of microwave heating is more efficient, which results in a shorter reaction time, lower energy consumption, and higher quality and yield products due to its nature of selective heating [2–4]. Microwave irradiation has been used for various applications, including organic synthesis reactions such as biodiesel and biolubricant [3,5–7]. Other than the thermal effect, some studies also claimed that microwave irradiation brings non-thermal effects, such as reducing the activation energy and enhancing the process's reactivity [8,9]. Due to these advantages, one future application of microwave-assisted transesterification would be to produce high-performance polyol ester biolubricant at a lower cost, as polyol ester production is typically expensive [10]. Currently, most available production technologies for polyol esters rely on conventional heating, which has several disadvantages, especially in terms of product quality and production cost.

Microwave heating is sensitive to frequency changes that could change the thermal field and produce different sizes, shapes, and locations of the hot spot. Aside from different heating material components,

* Corresponding author.
E-mail address: nuratiqah.aziz@gmail.com (N.A.M. Aziz).

https://doi.org/10.1016/j.rineng.2025.104577
Received 11 November 2024; Received in revised form 13 February 2025; Accepted 4 March 2025
Available online 7 March 2025

the specific location within the same substance could be heated selectively due to fluctuations in physical properties as temperature rises [11,12]. Yoshikawa et al. [11] stated that when temperature increased, local density, permittivity, magnetic permeability, and electric conductivity changed, resulting in a change in microwave absorbability. The change in microwave absorbability promotes accelerated local heating, which produces the hotspot. Hotspot may affect biolubricant quality. In a recent study [10], trimethylolpropane (TMP) triester was synthesized under microwave irradiation, and it was found that microwave technology can significantly accelerate the transesterification process, reducing the reaction time from 1 h to 10 min. This showed that the transesterification was 3.1 folds faster in the presence of microwave irradiation. This was because of the volumetric heating mechanism offered by microwave heating.

Previous research has indicated that microwave heating of solid and liquid substances results in uneven thermal distribution [13,14]. The main reason behind this might be due to the non-homogeneous electromagnetic field distribution within the microwave cavity as a result of wave reflections and interference. Moreover, the intense microwave heating at the top surface of the sample is due to the uneven electromagnetic distribution [15,16]. The wave reflects within the cavity, causing some locations to have high intensity and some locations to have low intensity [14]. Satpathy et al. [17] observed hotspot and localized initiation of the reaction in their work on microwave-assisted torrefaction of biomass, which was attributed to the selective heating mechanism of microwave irradiation, the non-homogeneous nature of the samples, the unequal distribution of the electric field, and the use of non-optimal microwave irradiation. In another study, the interaction of biomass with microwave was evaluated using a mode stirrer and bottom-fed microwave guide feature [18]. Bottom-fed waveguides had poorer electromagnetic wave distribution than side-fed waveguides (domestic oven). Song et al. [19] evaluated hot and cold spots of blackberries after microwave-vacuum drying for 2 min. Both simulation and experimental results demonstrated that the cold spot in the cavity's center emphasizes the non-uniform heating of microwave heating.

In recent years, considerable effort has been made in the multiphysics field of numerical simulation to understand microwave heating better. Ong et al. [20] investigated the non-catalytic transesterification for biodiesel production under the microwave using a commercial finite element method (FEM) software. The presence of hotspots, heat transfer from the inner layer to the outer layer, and non-homogeneous temperature and electric distribution profile were all observed. The simulation confirmed that the microwave cavity was well-designed because it reflected only 6.6 % of microwave energy back to the waveguide and could convert 75 % to thermal energy. In a different study, Yeong et al. [21] also reported the microwave conversion of palm fatty acid distillate to biodiesel. The effects of electromagnetic propagation, heat transfer, fluid flow, and chemical species conservation have been successfully described with the consideration of methanol and water vaporization. In general, previous simulation studies provided critical insight into the effect of microwaves on the esterification process, which could be used to optimize the reaction under the microwave effect. The available references on microwave heating simulations are more limited to the coupling of *emw* and *ht* modules, while the coupling of *emw, ht* and *re* modules is still scarce. Hence, in this study, the *re* module was integrated into the modelling to improve the prediction of concentration profiles of the transesterification products.

Although numerous studies were conducted on microwave-assisted transesterification reactions to produce biodiesel, there is a lack of research on microwave-assisted biolubricant production, particularly using a multiphysics-based modelling approach to gain better insight. Modelling could be used to determine the heating behavior of ester under microwave heating, to better understand the phenomena of heat transport, the distribution of the electric field, and the power absorbed by the sample in the oven cavity. This analysis would also be useful for the industrial design of microwave reactors for biolubricant production. The lack of this knowledge may hinder the upscaling of reactors and the understanding of the fundamentals of microwave heating. Therefore, this study aimed to simulate microwave-assisted biolubricant production using coupled electromagnetic wave-heat transfer-chemical reaction models to simulate the formation of hot spots and investigate the electric field and power distribution during the reaction.

2. Materials and methods

A model to simulate the transesterification reaction of (trimethylolpropane) TMP and (palm oil methyl ester) PME under microwave irradiation was constructed. Several modules were used in the model, such as reaction engineering (*re*), electromagnetic waves (*emw*), and heat transfer in fluids (*ht*). First, the *emw* was defined accordingly to solve the distribution of the electric field and forward the results to the *ht* module. Finally, the *re* module was solved by predicting the concentration profile of the transesterification reaction. The fields were solved using the Finite Element Method (FEM).

- The **electromagnetic field** is solved using Maxwell's equations in the frequency domain to account for microwave interactions with the reactor.

  Electromagnetic field: Eq. (1)

- The **thermal field**, solved using the heat conduction equation to capture temperature distributions within the reactor.

  Heat transfer: Eqs. (12) and (13)

- The **chemical reaction field**, involving the kinetics of polyol ester formation, was solved using approximate rate equations derived from Aziz et al. (2020). These equations were integrated into the thermal field solution as source terms for heat generation and material consumption.

  Chemical reaction engineering: Eqs. (15), (16), (17), and (18).

While other equations are cited from the literature (White, 1970); Eqs. (2), (3), (4), (5), (6), (7), (8), (9), (10), and (11).

A simulation study on microwave irradiation with reaction was conducted using numerical modelling software (COMSOL Multiphysics 4.2 software) to solve the complex numerical problems in the system. This helps to understand the governing transport phenomena and heat transfer efficiency under microwave conditions. The model was developed according to the following assumptions:

1. The reactant mixture is assumed to be a homogeneous single-phase solution
2. The dielectric properties of the reactants have marginal variation with temperature. It could be assumed to be constant throughout the reaction [21].
3. The air is microwave-transparent ($\varepsilon'=1$) [21]. The temperature of the air surrounding the reaction medium is constant during the reaction.
4. The vacuum condition of the reaction is neglected.
5. The catalyst sodium methoxide was omitted from the model since it was not consumed nor produced during the reaction.
6. During the reaction, the temperature at the measurement point was assumed to be isothermal.
7. The whole reaction system is perfectly symmetrical.
8. No heat is lost to the surroundings as the microwave reactor is perfectly insulated.

The domain for the model consists of the microwave oven cavity and a liquid mixture sample. The liquid sample constituted the flask shape and was placed at the center of the oven. A rectangular box at the side of

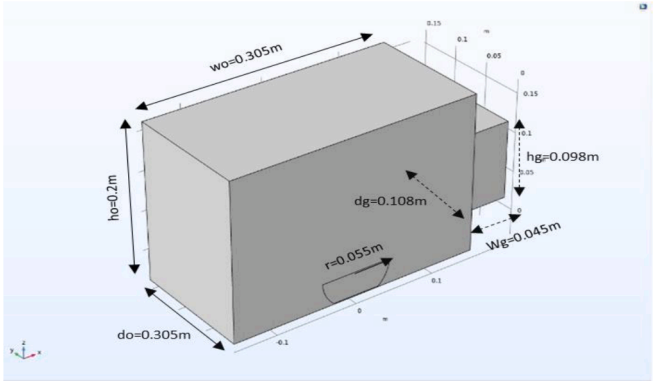

Fig. 1. Transesterification model for COMSOL simulation.

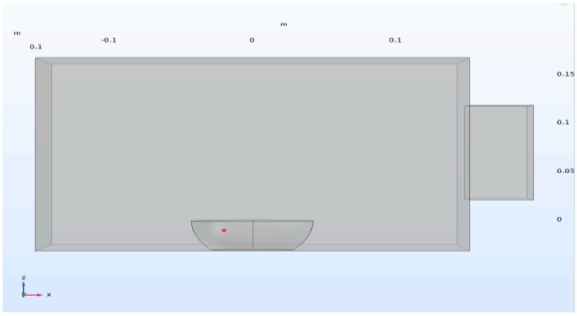

Fig. 2. Temperature measuring point.

the microwave oven represented the waveguide or port, as in Fig. 1. In the experiment, a thermocouple probe was used to measure the temperature profile of the mixture at a fixed location. The Cartesian coordinates for this point is −0.02 m (x) × 0.015 m (y) × −0.012 m (z), as shown in Fig. 2.

The materials involved in the model were selected from the built-in material in COMSOL software for copper and air. The data for PME and TMP were taken from experimental work and ASPEN PLUS tools. The microwave oven was made of copper, while the reactor was made from borosilicate glass. Because the borosilicate glass is transparent to the electromagnetic wave, it is omitted from the model. The flask half-form defines the liquid domain in the COMSOL model. If a full three-neck flask is built, it will be described as an impedance boundary with air properties (which will not participate in the heating of the liquid) [22]. According to Wang et al. [23], the dielectric loss of borosilicate glass is around $10^2 - 10^3$. All material properties are provided in Tables 1–3. The properties of copper and air were obtained from the COMSOL library, while the mixture was analyzed as in the previous study [24].

The magnetron that supplies the electromagnetic wave for a domestic microwave oven operating at 2.45 GHz was set to 480W. The wave was propagated in the z-direction from a waveguide cavity of 10.8 cm (W) x 9.8 cm (H). The microwave dimension is 30.5 cm (L) x 30.5 cm (W) x 20 cm (H). Other important parameters are tabulated in Table 4. The inside of the microwave reactor and the cavity were filled with air. The coarse free tetrahedral mesh of the drawing was assigned to all domains for faster and shorter computation time. The simulation was conducted on a 3 GHz Windows workstation with 24 GB memory. Among the modules applied were electromagnetic waves (*emw*), heat transfer (*ht*), and reaction engineering (*re*).

Table 1
Properties of copper.

Properties	Value	Unit
Relative permeability	1	1
Electrical conductivity	5.998×10^7	S/m
Relative permittivity	1	1

Table 2
Properties of air.

Properties	Value	Unit
Relative permittivity	1	1
Relative permeability	1	1
Electrical conductivity	0	S/m

Table 3
Properties of the mixture.

Properties	Mixture	Unit
Dynamic viscosity	0.00823	Pa.s
Density	914.87	kg/m³
Thermal conductivity	0.1067	W/(m·K)
Heat capacity at constant Pressure	2388.94	J/(kg·K)
Electrical conductivity	0.0375	S/m
Relative permeability	1	1
Relative permittivity	3.25–0.27j	1
Ratio of specific heats	1.1	1

2.1. Electromagnetic wave (emw) module

An electromagnetic wave *(emw)* module was constructed to solve time-harmonic electromagnetic field distribution. This wave equation is solved using the Maxwell equation to obtain the electric field value. The input data for this equation was from the dielectric properties defined in the material section. By solving the *emw* module, the value is carried forward for solving *ht* and *re* modules. Three domains selected were the oven cavity, waveguide and the sample. From this module, the electric field distribution across the oven was obtained. Considerations made throughout the modelling are:

1. The walls of the rectangular cavity of the microwave oven, the waveguide and the symmetry plane were assumed to be a perfect electric conductor. The tangential component of the electric field, $E_{tangential}$, oven wall was set to zero, $\nabla \cdot E = 0$.
2. The microwave oven walls were assigned for thermal insulation at which there is no heat flux across the boundary, $\nabla(k\nabla T) = 0$

In COMSOL, the metallic part of the oven was defined as a perfect electric conductor (PEC) boundary. This boundary condition is a lossless surface that reflects all incident waves. Copper has a higher thermal and electrical conductivity than other metals and can be used as an ideal situation in the early stages of model development to see how well a device would perform without material losses. The value of the electric field inside the cavity is essential to obtain volumetric power density inside the sample. Maxwell's equation in Eq. (1) is the equation for solving electromagnetic problems in COMSOL. μ_r is relative permeability, E is the electric field (Vm^{-1}), ε_r is relative permittivity, ε_o is constant permittivity in a vacuum, 8.854×10^{-12} (F/m), and σ is electric

Table 4
Dimension for COMSOL simulation.

Description	Value	Unit
Average total density	896.1	kg/m³
Molecular weight of TMP	0.13417	kg/mol
Molecular weight of PME	0.29489	kg/mol
Molecular weight of TMPME	0.39706	kg/mol
Molecular weight of TMPDE	0.65991	kg/mol
Molecular weight of TMPTE	0.92275	kg/mol
Molecular weight of Met	0.03204	kg/mol
Volume of mixture	1.5×10^{-4}	m³

conductivity (S/m). By solving this equation using Finite Element Method (FEM) with COMSOL Multiphysics software, the electric field distribution within the microwave reactor was simulated.

$$\nabla \times \frac{1}{\mu_r}(\nabla \times E) - k_o^2\left(\varepsilon_r - \frac{j\sigma}{\omega\varepsilon_o}\right)E = 0 \quad (1)$$

$$\varepsilon_r = \varepsilon_r{}' - j\varepsilon_r{}'' \quad (2)$$

$$\tan\delta = \frac{\varepsilon_r{}''}{\varepsilon_r{}'} \quad (3)$$

Microwave heating is highly dependent on a material's dielectric properties as it defines a sample's ability to absorb and convert microwave energy into heat energy. Generally, the dielectric properties of a material can be shown as Eq. (2). It is a complex number with (j) imaginary part, the dielectric loss ($\varepsilon_r{}''$), determining how much microwave energy is being converted into heat; and (ii) the real part, the dielectric constant/relative permittivity ($\varepsilon_r{}'$), showing a material's ability to store microwave energy. The dielectric properties can also be described as dielectric loss tangent, as shown in Eq. (3).

2.2. Heat transfer (ht) module

The boundary for the thermal insulation node was selected to determine whether there was any heat loss area. The node was automatically added to the *emw* module. So, another node heat flux was chosen to specify which boundaries have heat loss conditions. As the wave travels in a sample, the energy dissipated $|E|$ in the sample drops and appears as heat. Maxwell's equation solved the magnitude of a peak value of the electric field, E, of the model at any location. From the electric field obtained, the power absorbed per volume of sample (W/m^3) was calculated using the following Eq. (4) [25]:

$$\frac{P}{V} = 2\pi f\varepsilon_o E^2\varepsilon_{mix}'' \quad (4)$$

$$E = \frac{3E_0}{(\varepsilon_{mix}' + 2)} \quad (5)$$

$$\varepsilon_{mix}' = x\cdot\varepsilon_{TMP}' + (1-x)\cdot\varepsilon_{PME}' \quad (6)$$

$$\varepsilon_{mix}'' = x\cdot\varepsilon_{TMP}'' + (1-x)\cdot\varepsilon_{PME}'' \quad (7)$$

Where f is microwave frequency; 2.45 GHz, ε_o is the permittivity of vacuum, 8.854×10^{-12} (F/m), E is electric field intensity, (V/m), and $\varepsilon_{\text{mix}}''$ is the average dielectric loss of the sample. The experimental power absorbed was calculated from the relationship of the electrical field inside the sample to the electric field outside the sample, E_o. The equation was as follows in Eq. (5) [25].

The average dielectric constant of the sample, $\varepsilon_{\text{mix}}'$ and average loss factor $\varepsilon_{\text{mix}}''$ were estimated as assumptions made as follows:

1. The reactants consist of TMP and PME.
2. The product comprises TMPTE, TMPDE, and the excess reactant, PME. TMPME was present in traces and did not affect the dielectric properties.
3. ε' and ε'' for each product were taken at room temperature, and they are assumed constant at increasing temperature. In this study, the electromagnetic field was computed assuming constant dielectric properties of the reaction medium. This assumption is based on prior studies by (Rajab et al., 2011) indicating that the dielectric constant of palm oil changes minimally within the 25 to 100 °C temperature range relevant to the reaction. For instance, (Rajab et al., 2011) reported that the dielectric constant of palm oil varied by 0.9 % across 25 to 100 °C, which is unlikely to influence electromagnetic field distributions or energy absorption patterns significantly. While this approach simplifies the computational model, we acknowledge that temperature-induced variations in dielectric properties could become significant in scenarios involving wider temperature ranges, different materials, or highly sensitive field configurations.
4. The components presented at the beginning of the reaction were TMP and PME. Thus, the average dielectric properties for the mixture at the initial stage of the reaction were calculated as follows. x is the composition of the component:

Before using both Eqs. (4) and (5), the water load method was implemented to estimate the value of the electric field outside the sample, E_o in the microwave. A 250 ml spherical flask was filled with 50 mL distilled water and placed at the microwave centre-base cavity. The water temperature was 5 °C below room temperature (25 °C). The microwave was set at full power (800 W) for 30 s. The final temperature after the run was recorded. The average power absorbed by water was obtained based on Eq. (10):

$$\frac{P}{V} = \frac{c_p\cdot\rho_w\cdot\Delta T}{\Delta t} \quad (8)$$

C_p of water: 42000J/kg· °C, ρ of water :1000kg/m^3

$$\frac{P}{V} = 2\pi f\varepsilon_o E^2\tan\delta\ \mathrm{K} \quad (9)$$

Loss tangent, tanδ = ε''/ε': 0.160 (acceptable range is 0.1–0.17)

K is a relative dielectric constant of water, which, in the 2.45 frequency range at temperature moderately above room temperature, is 72.

$$E_0 = \frac{k+2}{3}\mathrm{E} \quad (10)$$

Rectangular Port has an input power of 480 Watt (60 % of microwave output power). The microwave heating effect is a function of the absorbed electric field and the dielectric loss factor. During the experiment, the microwave heating supplied is in pulsed heating, obtained when the microwave power was at 480 W, switched on for 12 s and switched off for 8 s. The heat source imitates a cyclic pattern by multiplying the electromagnetic heat source term with a periodic piecewise function, as in Eq. (11).

$$\mathrm{QMW} = \begin{cases} 2\pi f\varepsilon_0\varepsilon_r{}''\,E^2 & \text{if } 0 \le t < 12 \\ 0 & \text{if } 12 \le t \le 20 \end{cases} \quad (11)$$

A piecewise function from the global definition was selected and defined as below:

Argument: x

Extrapolation: Periodic

Smoothing: No smoothing

The intervals were defined as below:

Intervals

Start	End	Function
0	8	1
8	20	0

For the Port subset under the Electromagnetic waves tab, a rectangular port was selected with enabled wave excitation at the port. A transverse electric (TE) mode-type port was chosen.

The domain for heat transfer in the fluid module is only the sample. The properties of the mixture were comprised of the average value of TMP and PME's properties (average density, average heat capacity, average thermal conductivity, average electrical conductivity, etc.). The temperature rise in the reaction solution is obtained from Fourier's law:

$$\rho c_p \frac{\partial T}{\partial t} + u = \nabla(k\nabla T) + Q_{MW} + Q_{\Delta H} \tag{12}$$

$$Q_{\Delta H} = \Delta H_r R \tag{13}$$

Eq. (12) was obtained from COMSOL, where ρ is density, *Cp* is the specific heat capacity of the medium (J/(kg·K), k is the thermal conductivity, u is the internal energy and Q is the heat source or sink (W/m^3). T is the absolute temperature (K), u is the internal energy (W/m^2), and p is pressure (Pa). Q_{MW} is a function of the absorbed electric field and the dielectric loss factor. The enthalpy change occurs as the reactants are transformed into products through transesterification (endothermic). The changes introduce a heat sink, $Q_{\Delta H}$, into the system, and $\dot{R}$ is the heat of the reaction, expressed in Eq. (13).

2.3. Chemical reaction engineering (re) module

The overall reaction of a transesterification reaction in Eq. (14) comprises three elementary reversible series-parallel reactions. The rate law expressions are given in [26]. The reaction rate in the COMSOL (*re*) module was specified as temperature-dependent, thus connecting the microwave heat source from the *emw* module with the *re* module.

$$TMP + 3\ PME \leftrightarrow \text{TMPMonoester} + \text{TMP Diester} + \text{TMP Triester} + 3\ \text{Methanol} \tag{14}$$

$$\frac{dc_i}{dt} = R_i = v_i r \tag{15}$$

$$r_j = k_j^f \prod_{i=1}^{Q_r} c_i^{-v_{ij}} - k_j^r \prod_{i=1}^{Q_p} c_i^{v_{ij}} \tag{16}$$

$$k^f = A^f \left(T/T_{ref}\right)^{n^f} exp\left(\frac{-E^f}{R_g T}\right),\ T_{ref} = 1K \tag{17}$$

$$k^r = k^f \Big/ K_{eq_0} \tag{18}$$

Eqs. (15)–(18) are the general equations used in COMSOL already described under the kinetics modelling section. Eqs. (15) and (16) are the expressions to obtain the reaction rate constant, while Eq. (17) refers to the Arrhenius equation for activation energy estimation. Eq. (18) is to specify the forward rate constant for the reactions. By selecting *re* modules, the system was assumed to be in perfect mixing. The reaction engineering module was solved using the average temperature method, as it provides a representative value for the reaction kinetics. The reactor used in this study is small (<100 mL of working volume) and stirred throughout the reaction. From this, the reactor is assumed to have perfect mixing and averaged temperature. This choice simplifies computation while still capturing the overall energy distribution effects.

3. Results and discussions

3.1. Simulation of heat transfer during transesterification of palm oil methyl ester (PME) and trimethylolpropane (TMP)

The governing transport phenomena and heat transfer parameters of microwave reaction were modelled using COMSOL Multiphysics 4.2 software. A fully coupled electromagnetic - heat transfer – chemical reaction model for transesterification reaction was employed. The model consists of 3 modules which are modules for electromagnetic wave (*emw*), heat transfer in fluid (*ht*), and reaction engineering (*re*) modules. Two study steps of analysis involved were frequency domain and time dependent. For solving the *emw* module, the frequency domain is necessary, while other modules were solved in a time-dependent study stage. A module was solved step by step by the COMSOL solver and the results were used to solve the following modules (*emw*→ *ht*→ *re*). To shorten the computation time, coarse meshing was chosen for the model. A physic-controlled mesh was selected in the setting so that COMSOL Multiphysics created a mesh that can be adapted to the current physics interphase settings. The frequency of the model was set at 2.45 GHz, which is similar to the experimental condition. Fig. 3 shows the meshing scheme of the model. The average element quality for the model mesh's coarse, normal, and fine sizes is 0.6457, 0.6476, and 0.6562, respectively, for a mesh volume of 0.009558 m3. The results showed that the electric field distribution and the power density were consistent across all mesh configurations, with deviations of <2 % in the key parameters.

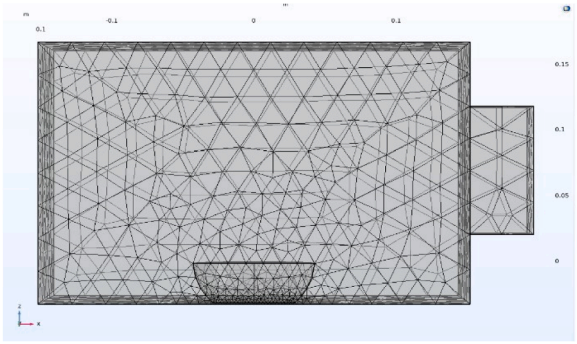

Fig. 3. Meshing scheme implemented in the modelling.

3.2. Prediction of reaction rate of the transesterification reaction

This section provides an insight into the simulated yield of the product achieved using the reaction engineering (*re)* module in the COMSOL. Concentration profiles were obtained at four different temperatures (110, 120, 130, 140 °C). The reaction rate constant (*k*), 3.264 × 10^{-6}, 1.518 × 10^{-6}, 1.1503 × 10^{-6}, 9.7402 × 10^{-8}, 7.3984 × 10^{-7}, and 1.9532 × 10^{-7} m^3/(s·mol) for *k1, k1r, k2, k2r, k3* and *k3r,* respectively was obtained from the previous kinetics study [26]. The initial concentration converted the mass fraction to a concentration unit of 2813 mol/m^3 and 666 mol/m^3 of PME and TMP, respectively. Fig. 4. shows the predicted concentration of the limiting reactant TMP and the products during the reaction. The TMP concentration is high at the beginning of the reaction, indicating that the TMP is yet to be consumed. Over time, the concentration of TMP decreased while the reaction products, which are TMPME, TMPDE, and TMPTE, increased. Fig. 4 shows that the product concentration may not reach equilibrium within the simulation time of 25 min (1500 s). The TMPTE curve is still increasing while the limiting reactant is finishing halfway, resulting in a gradual decrease in the production of TMPTE. The reaction in Fig. 4(a) shows the lowest consumption of TMP compared to other reactions, which may be due to insufficient energy at a temperature reaction of 110 °C. Since the TMP was not fully reacted, the production of intermediate products (TMPME and TMPDE) was low. The increase in temperature to 120 °C in Fig. 4(b) results in an improvement in the yield of TMPME from TMP. However, the energy is not enough to continue to the second (to produce TMPDE) and third step (to produce TMPTE) due to insufficient heat applied to the system.

Next, the concentration profile of reactions at 130 °C and 140 °C

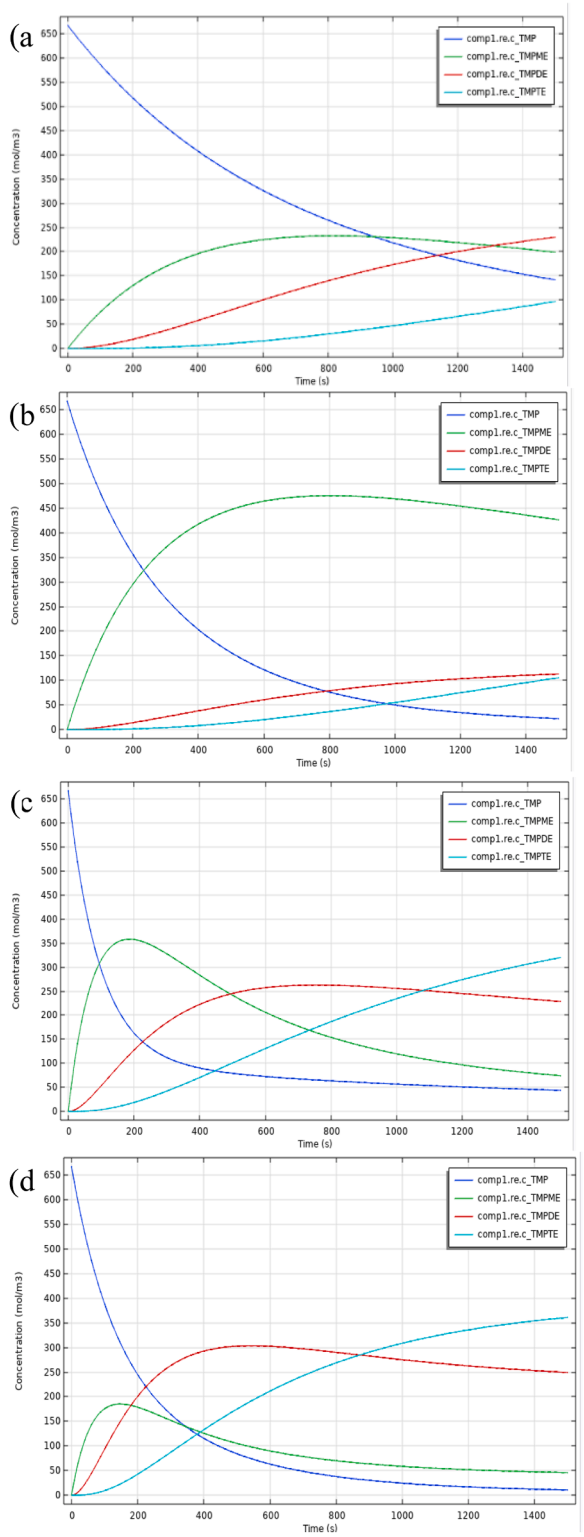

Fig. 4. Predicted concentration profile by COMSOL at (a) 110, (b) 120, (c) 130, and (d) 140 °C.

(Fig. 4(c) and (d)) shows a similar trend, where the TMP is quickly consumed until approximately 200 s and the production of TMPTE is high. This indicates that a temperature above 130 °C may be required to produce a high yield of TMPTE. The results are consistent with the kinetic results, which suggested that the temperature of 130 °C was optimal for the transesterification of TMP and PME. However, from the COMSOL simulation results, the concentration of TMPDE at 140 °C was higher but may not be preferable because it may reduce the viscosity of the final product [27,28].

This simulation model, however, has some limitations that could affect the accuracy of the results. For instance, it was observed that the simulated reaction took 25 min to be considered complete. While the experimental reaction was at an optimum condition of 10 min. The limitation of the model has been contributed by:

1. The reaction was in atmospheric conditions (not in a vacuum), which means that methanol was not removed from the system. When this condition is applied, the reaction rate is slower because there's no driving factor to the forward direction of the reaction. Besides that, the boiling points of the reactants were not reduced without a vacuum.
2. The change in phase of the TMP was not considered in the system.
3. The average desired temperature of the mixture was lower, which affected the reaction temperature and, therefore, the reaction rate.

Nevertheless, the simplification of the *re* module was still valid because the objective of this module was to understand the effect of temperature on the distribution of transesterification products of TMP and PME using the microwave. It was found that the temperature of 130 °C which has k values $k1$, $k2$, $k3$, $k1r$, $k2r$, and $k3r$ of 3.264×10^{-6}, 1.518×10^{-6}, 1.1503×10^{-6}, 9.7402×10^{-8}, 7.3984×10^{-7}, and 1.9532×10^{-7} $m^3/(s\cdot mol)$, respectively, is required to produce sufficient energy for the reaction to take place satisfactorily [26].

3.3. Electric field distribution in the oven and sample

In microwave heating, the distribution of the electric field is affected by sample dielectric properties, sample volume and microwave frequency [21,29,30]. In this study, the input power was 480 W, based on the fabricated microwave's actual power cycle. In an empty microwave oven, the typical electric field distributions are organized in all the planes, and the hot and cold spot regions should be distinguished [21].

The magnetron produced microwave at 2.45 GHz, travelled via the rectangular waveguide, and entered the microwave oven cavity. The strong heating at red spot regions near the waveguide was induced by the microwave reflection from the metallic wall and interference with the incident microwave from the magnetron [20]. To save computing time, the drawing of the symmetrical geometry model was cut to half in the later computation. Fig. 5(a), (b), and (c) show the electric field distribution of the empty oven from the front, top and side view, at 2.45 GHz, respectively, as a control. It is observed that the electric field is uniform with the destructive and constructive nature of the waves in the oven, which is also known as the interference phenomenon [20]. Destructive and constructive interference of microwaves creates hot (red) and cold (blue) spot regions, consistent with Yeong et al.'s [21] previous study.

Once the sample was placed in the oven, the distribution of the electric field changed, as shown in Fig. 5(d), (e), and (f) displaying the front, top and side view of the microwave, respectively. It was observed that the electric field was severely disturbed as the sample was placed in the oven. The electric field intensity was observed at the top corner of the sample. This occurred because the reaction mixture, trimethylolpropane ester (TMPE), absorbed the energy of the microwave, thereby altering the overall strength of the electric field.

It should be noted that the experiments were carried out exclusively at 2.45 GHz utilizing the domestic microwave frequency. Electric field distribution is affected by the microwave frequency [22]. Furthermore, microwave frequency may influence temperature distribution within the sample [22,31]. Although the effect of frequency on electric distribution was not tested experimentally, a frequency variation was used in the simulation to gain some insights into the distribution of the electric field profile at different microwave power intensities. Different electric field profiles were observed when 2 GHz and 4 GHz were applied to the

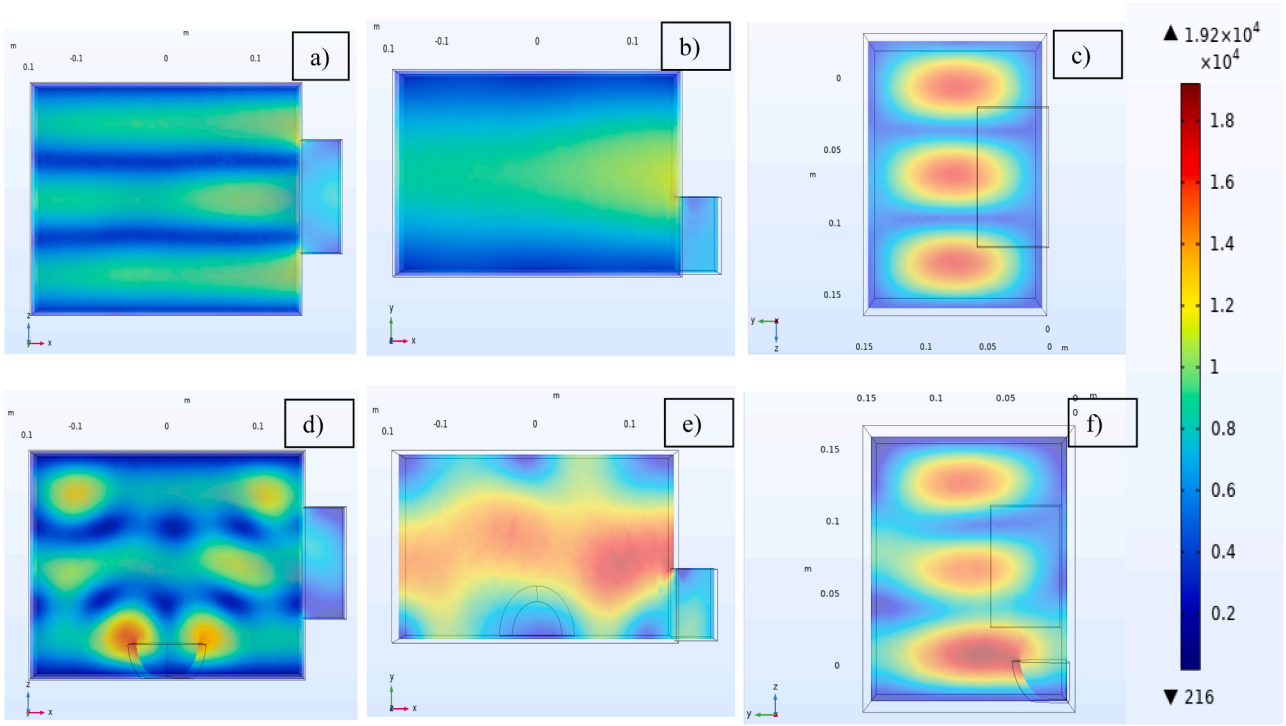

Fig. 5. Electric field distribution (V/m) in the empty microwave oven from the (a) front, (b) top and (c) side view at 2.45 GHz and with a sample from the (d) front, (e) top and (f) side view at 2.45 GHz (Half drawing).

model, as presented in Fig. 6. The electric profile of the oven at 2 GHz shows a moderate intensity on average, based on the yellowish colour profile. A low frequency with a long wavelength corresponds to a greater microwave penetration depth in comparison to the depth of the sample. In theory, a large portion of microwaves can pass through the sample. The wave was then reflected at each interface, from air to the top and lower surfaces of the sample and back to air. These reflection and transmission components at each interface contributed to the resonance of a standing wave configuration within the sample, resulting in a microwave absorption peak farther from the incoming microwaves' surface [32]. Lower microwave frequencies will result in lower heating temperatures and insufficient energy for high TMPTE yield. Moreover, the domestic oven is usually equipped with a 2.45 GHz magnetron, so the simulation model has also been set at the same frequency.

A higher microwave frequency of 4 GHz was also applied, and the results are presented in Fig. 6(d) – (f). The electric field has been observed to be intense and faster – narrower wavelength. High frequency has a short wavelength, which means that a stronger standing wave with a large amplitude is formed by interference between the incident and the reflected waves from the surface of the sample [31,33]. This frequency may be too high to be applied to the model, resulting in higher electric field intensity and eventually affecting the final temperature of the mixture and the quality of the final product.

The electric field (V/m) and the distribution of the power density (W/m^3) in the mixture (TMPE) at 2.45 GHz are shown in Fig. 7 below. The heat transfer coefficient represents the dielectric constant and dielectric loss (or loss factor) for this research study. The dielectric constant is the ability of a material to store energy, and the loss factor is the ability of a material to dissipate heat or energy. P/V represents the electric field. White et al., 1970 introduced the power-to-volume relation as in Eq. (9) and loss tangent, $\tan\delta = \varepsilon''/\varepsilon'$. In Fig. 2, the red dot indicates the presence of a thermocouple. Based on the COMSOL image in Fig. 8, the electric field is higher near the k-type thermocouple than in other locations. The result implied that the heat dissipation in the area was more efficient; hence, the loss factor, as indicated by the loss tangent equation near the thermocouple, is higher than in other locations.

The maximum value of the electric field was 1.92×10^4 V/m, while the maximum power density in the TMPE was 1.38×10^7 W/m^3, as in Fig. 8. These values are comparable to the previous study in the production of biodiesel using microwave [21,22]. In the production of biodiesel using a microwave by Yeong et al. [21], the power absorbed by the sample was 1.38×10^6 W/m^3. This difference was due to the difference between the study's reaction materials, energy cycle, and microwave power supply. Previously, Yeong et al. [21] set the microwave power at 300 W for a 30-second energy cycle to reach 75 – 90 °C for biodiesel, which has a slightly lower complex relative permittivity (2.78–0.17j for PFAD) compared to the current material (3.25–0.27j for TMPE). In addition, the study established a lower microwave power for a longer cyclic time. The present study was set at 480 W of microwave power to reach 130 °C for 20 s of the energy cycle. This condition explained why the power absorbed by both studies was somewhat different.

In order to validate the model constructed for the *emw* module, the electric field and the water-absorbed power (as a control group) were experimentally measured using the same microwave reactor, based on Eqs. (4)–(10). The electric field was found to reach 7.01×10^4 V/m with an absorbed power of 8.3×10^7 W/m^3. Compared with the electric field of TMPE calculated by COMSOL, which is 1.92×10^4 V/m, the electric field of water is 72.6 % higher. This may be due to the specific complex relative permittivity of water and ester, 78–12.5 j and 3.25- 0.27j, respectively. The polarity of water is higher than that of ester. High polarity means that the water tends to absorb more energy and be influenced by microwaves, thus recording a high electric field and power in the sample. The power density originating from the energy supply of the microwave to the reaction mixture was set to be in cyclic function as Eq. (11). The reaction reached a desired temperature of 130 °C after approximately 3 min. This is similar to the experimental value of the optimum heating duration. The sample was supplied with microwave power during the reaction until it reached 130 °C (optimum conditions). At 130 °C, the microwave stopped providing the additional power following the cyclic pattern and heat source function described earlier.

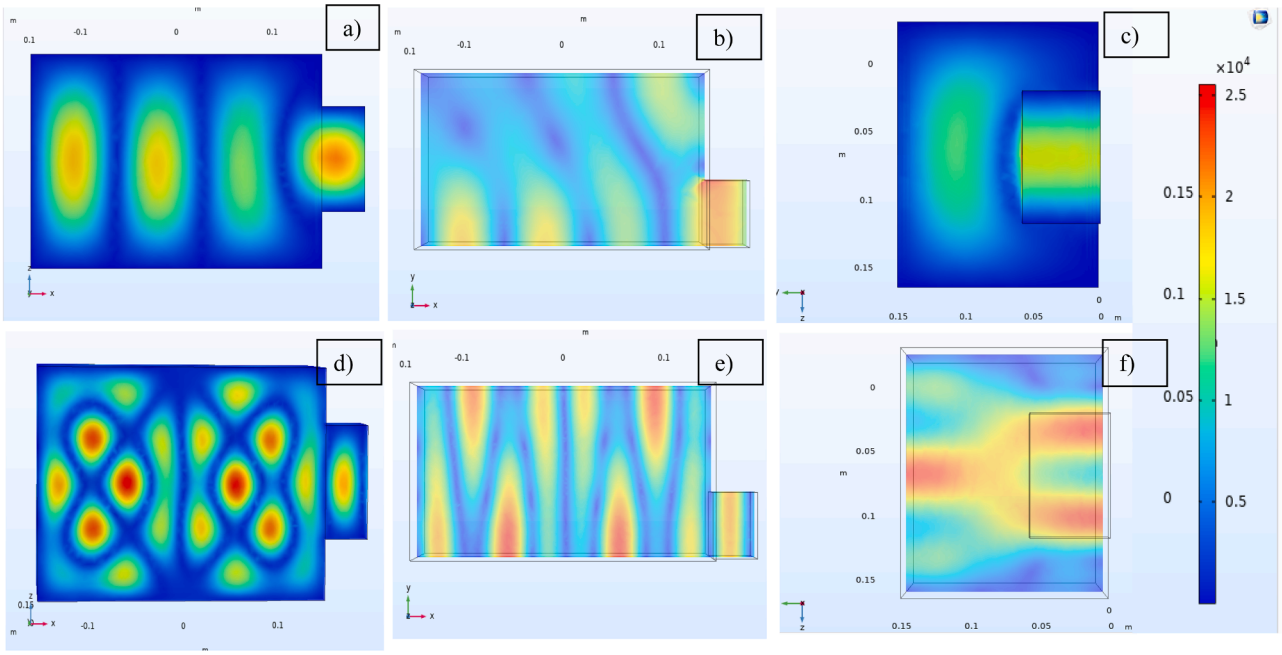

Fig. 6. Electric field distribution (V/m) in the empty microwave oven from the (a) front, (b) top and (c) side view at 2 GHz and from the (d) front, (e) top and (f) side view at 4 GHz (Half drawing).

Solving *emw* module provided a series of electric profiles to visualise and quantify microwave-TMPE interaction. The results showed that the microwave absorption by TMPE induced a significant redistribution of the electromagnetic field in the oven cavity. As indicated earlier, high- and low-energy regions have been formed. The distribution of the electric field affects the microwave absorption and the accumulation of heat in the sample [34].

3.4. Heat transfer distribution in the sample (TMPE)

As previously established in the experimental results, sample heating in the microwave is significantly faster than conventional heating. The pre-heating time of conventional heating by means of an oil bath has been reduced from 40 min to 3 min using a microwave. Generally, the thermal gradient of conventional heating is transferred from the reactor (heating source) to the sample. Meanwhile, the distribution of the thermal gradient for microwave heating is from the inside to the outside of the sample. An electromagnetic wave is produced by a magnetron, which converts electric energy to radiation in a microwave oven, and

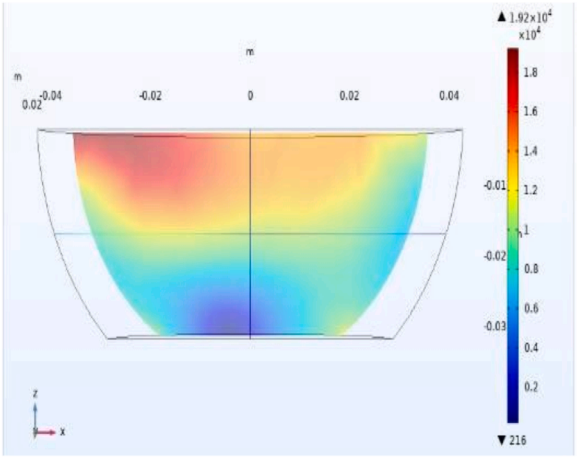

Fig. 7. Electric field (V/m) in TMPE.

then absorbed by the sample and converted to heat energy, which becomes part of the sample's internal energy. The power density absorbed by a sample in Eq. (4) was assessed by the electric field in Eq. (5) generated in the oven cavity. The ability of a sample to store absorbed energy and convert it into heat was attributed to its dielectric characteristics. Each material has a distinct dielectric property and depends on temperature, frequency, and moisture content. However, this study did not investigate the frequency and moisture content parameters. Convective heating is primarily associated with liquid samples. As heat was formed via dipolar polarisation and ionic conduction at microwave frequency, convective heating also occurred, with the top area of a sample consistently warmer due to the density difference. In this work, once the sample has achieved a temperature with adequate energy for reaction, an endothermic (transesterification) reaction occurs, which involves a heat sink in Eq. (13).

The simulation results from the *ht* module found that the heating was more intense at the top corner of the sample, which is in line with the previous electric field distribution in the *emw* module. Fig. 9 presents the temperature distribution during the transesterification reaction of this study. At different temperatures of 110, 120, 130 and 140 °C, the results showed a similar heat distribution with slightly higher temperatures in the upper left corner. The lowest temperatures inside the convective-heated liquid domain are likely near the glass reactor's bottom [35]. Temperature gradients form within the container as heat is generated, and warmer (lighter) liquid rises as the incoming microwaves constantly heat the liquid during the upward motion. Therefore, as the fluid flows further from the bottom, it becomes hotter, resulting in a high temperature in the upper region of the liquid domain [35]. The sample's location may be one reason for the heat distribution obtained. Compared to the previous study, Yeong et al. [21] placed the sample in the middle of the oven, where a stand was used to lift the position of the sample. Despite the irregular thermal gradient obtained, this non-uniform heating pattern, where the surface is hotter than the centre, is common in food heating using a domestic oven.

Ryynanen et al. [36] studied hamburger heating in the domestic microwave oven. It was found that each layer was heated differently, and the surfaces and edges were warmer. A similar phenomenon was observed by Zhao et al. [37] in a study of microwave heating of water in

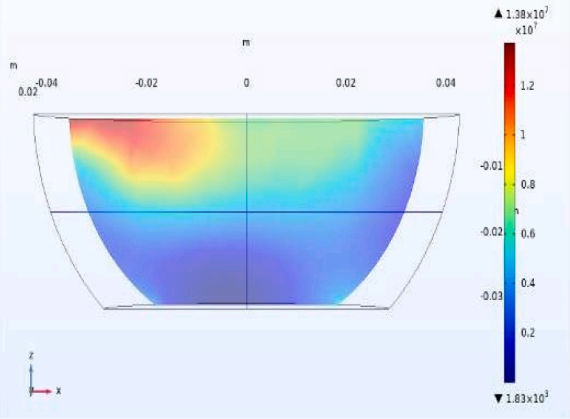

Fig. 8. Power density distribution (W/m^3) in TMPE.

glass. The top part of the glass was warmer than the bottom half. Zhao et al. [37] pointed out that the attenuation of the microwave from the waveguide could result from the electromagnetic waves at a cut-off frequency. Therefore, this study's findings are acceptable and in line with previous studies.

The dielectric properties of each sample layer affected the heating profile. The dielectric properties of the sample have led to microwave absorption and heat conversion. The strength of the reflected wave and the reduction of microwave penetration depth of the substance also depends on its dielectric properties [36]. The other factor contributing to the hotter surface area or higher microwave power absorbed on the surface is the penetration depth of the microwave. Rattanadecho et al. [32] classified 2.45 GHz as a high-frequency wave resulting in a short wavelength. The short wavelength gave a shorter depth of penetration. Wave reflection may change the power density quotients when some fields have been cancelled due to destructive interference. At the same time, some fields have been amplified due to constructive interference in the microwave oven. In this case, the microwave could have penetrated from the top corner of the mixture surface and finally reached the bottom, as our system was small.

From the final form of the Fourier's law-based continuity equation in Eq. (12), the heat loss term of TMPE in the microwave may include power due to microwave heating, *QMW* (1.38×10^7 W/m^3 or 2070 W) and reaction heat, $Q_{\Delta H}$ (11.97 kJ or 3.3 W). The convective effect of air in the thermally-induced free convection of microwave ovens was negligible, based on a previous study by Akarapu et al. [38]. Moreover, the evaporation of methanol was also not considered in the model. The power absorbed by the sample was sufficient to provide heat for the reaction at a short time, thus increasing the efficiency of the reaction in terms of time and yield. 70 % of TMPTE composition (98 % of TMPE) in 10 min was achieved for transesterification of PME and TMP using microwave heating.

In this study, the electromagnetic field was computed assuming constant dielectric properties, as the impact of temperature variations on these properties is minimal within the investigated range. Incorporating temperature-dependent dielectric properties through a fully coupled electromagnetic-thermal analysis may result in significant findings for future work.

4. Conclusions

A model that coupled three modules, electromagnetic waves, heat transfer, and chemical reaction engineering, demonstrated the profile of concentration, electric field, and temperature. The phenomena of heat transport from microwave radiation to heat generation were successfully investigated in this study. The distribution of the electric field in the oven associated with the hotspots, temperature profile and power

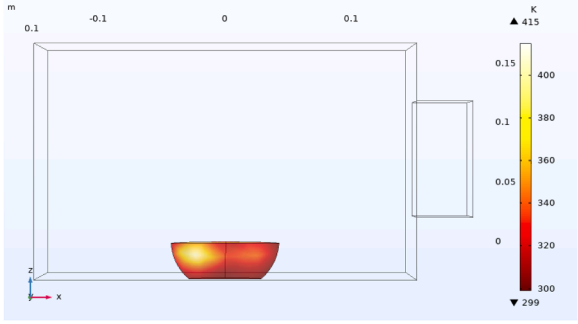

Fig. 9. Temperature distribution of mixture during transesterification reaction at 130 °C.

absorbed by the sample was assessed. Visualization and quantification of microwave-TMPE interaction were also achieved. The sample's electrical field and power absorbed were 1.92×10^4 V/m and 1.38×10^7 W/m^3, respectively. The effect of temperatures on the distribution of TMP and PME transesterification products using microwave was successfully simulated using COMSOL. A temperature of 130 °C was required to produce sufficient energy. The visualization and quantification of microwave-TMPE interaction showed a significant redistribution of the electromagnetic field in the oven cavity. The heating behaviour of TMPE during the transesterification reaction using a microwave was identified to be intense at the top corner of the sample.

CRediT authorship contribution statement

Nur Atiqah Mohamad Aziz: Writing – original draft, Investigation, Conceptualization. **Hassan Mohamed:** Supervision, Funding acquisition. **Mei Yin Ong:** Writing – review & editing. **Robiah Yunus:** Supervision, Resources. **Ming Chiat Law:** Writing – review & editing, Supervision. **Hamidah Abd Hamid:** Writing – review & editing. **Dina Kania:** Writing – review & editing. **Teuku Meurah Indra Mahlia:** Writing – review & editing, Supervision, Resources.

Declaration of competing interest

The authors declare that they have no known competing financial interests or personal relationships that could have appeared to influence the work reported in this paper.

Acknowledgement

The authors would like to express gratitude to Universiti Putra Malaysia for providing Putra Graduate Initiative Grant (IPS) (Vote No.: 9580200) and conducive research facilities. The authors would also like to acknowledge Ministry of Higher Education, Malaysia and UNITEN for supporting this study using the Higher Institution Centre of Excellence Fund [JPT.S(BPKI)2000/016/018/015Jld.4(21)/2022002HICOE]; as well as Akaun Amanah Industri Bekalan Elektrik (AAIBE) Chair of Renewable Energy [202004KETTHA]; Dato' Low Tuck Kwong International Energy Transition Grant [202203003ETG]; and UNITEN through Highly Cited Researcher (HCR) [BOLDREFRESH2025].

Data availability

No data was used for the research described in the article.

References

[1] N.A.M. Aziz, R. Yunus, D. Kania, H.Abd Hamid, Prospects and challenges of microwave-combined technology for biodiesel and biolubricant production through a transesterification: a review, Molecules. 26 (2021), https://doi.org/10.3390/molecules26040788.

[2] Z. Zhao, H. Li, K. Zhao, L. Wang, X. Gao, Microwave-assisted synthesis of MOFs: rational design via numerical simulation, Chem. Eng. J. 428 (2022), https://doi.org/10.1016/j.cej.2021.131006.
[3] J.J. Lin, Y.W. Chen, Production of biodiesel by transesterification of Jatropha oil with microwave heating, J. Taiwan. Inst. Chem. Eng. 75 (2017), https://doi.org/10.1016/j.jtice.2017.03.034.
[4] V. Amirthavalli, A.R. Warrier, B. Gurunathan, Various methods of biodiesel production and types of catalysts, Biofuels Bioenergy (2022), https://doi.org/10.1016/B978-0-323-85269-2.00020-4.
[5] H.A. Allami, M. Tabasizadeh, A. Rohani, A. Farzad, H. Nayebzadeh, Precise evaluation the effect of microwave irradiation on the properties of palm kernel oil biodiesel used in a diesel engine, J. Clean. Prod. 241 (2019), https://doi.org/10.1016/j.jclepro.2019.117777.
[6] A.S. Silitonga, A.H. Shamsuddin, T.M.I. Mahlia, J. Milano, F. Kusumo, J. Siswantoro, S. Dharma, A.H. Sebayang, H.H. Masjuki, H.C. Ong, Biodiesel synthesis from Ceiba pentandra oil by microwave irradiation-assisted transesterification: ELM modelling and optimization, Renew. Energy 146 (2020), https://doi.org/10.1016/j.renene.2019.07.065.
[7] J. Milano, H.C. Ong, H.H. Masjuki, A.S. Silitonga, W.H. Chen, F. Kusumo, S. Dharma, A.H. Sebayang, Optimization of biodiesel production by microwave irradiation-assisted transesterification for waste cooking oil-calophyllum inophyllum oil via response surface methodology, Energy Convers. Manage 158 (2018), https://doi.org/10.1016/j.enconman.2017.12.027.
[8] K. Huang, X. Yang, W. Hua, G. Jia, L. Yang, Experimental evidence of a microwave non-thermal effect in electrolyte aqueous solutions, J. Chem. 33 (2009), https://doi.org/10.1039/b821970b.
[9] W. Tian, Z. Li, L. Wu, Experimental demonstration of a microwave non-thermal effect in DMSO-NaCl aqueous solution, Chem. Phys. 528 (2020), https://doi.org/10.1016/j.chemphys.2019.110523.
[10] N.A.M. Aziz, R. Yunus, H.A. Hamid, A.A.K. Ghassan, R. Omar, U. Rashid, Z. Abbas, An acceleration of microwave-assisted transesterification of palm oil-based methyl ester into trimethylolpropane ester, Sci. Rep. 10 (2020), https://doi.org/10.1038/s41598-020-76775-y.
[11] N. Yoshikawa, G. Xie, Z. Cao, D.V. Louzguine, Microstructure of selectively heated (hot spot) region in Fe3O4 powder compacts by microwave irradiation, J. Eur. Ceram. Soc. 32 (2012), https://doi.org/10.1016/j.jeurceramsoc.2011.08.028.
[12] W. Wang, B. Wang, J. Sun, Y. Mao, X. Zhao, Z. Song, Numerical simulation of hot-spot effects in microwave heating due to the existence of strong microwave-absorbing media, RSC. Adv. 6 (2016), https://doi.org/10.1039/c6ra05191j.
[13] G. Brodie, The influence of load geometry on temperature distribution during microwave heating, Trans. ASABe (2008) 51, https://doi.org/10.13031/2013.25224.
[14] J. Zhou, Y. Li, N. Li, S. Liu, L. Cheng, S. Sui, J. Gao, A multi-pattern compensation method to ensure even temperature in composite materials during microwave curing process, Compos. Part a Appl. Sci. Manuf. 107 (2018), https://doi.org/10.1016/j.compositesa.2017.12.017.
[15] R. Zhong, L. Li, B. Yao, T. Xiang, Influence of convex spherical device on the local field distribution in the microwave reaction cavity, J. Phys. Conf. Ser. (2022), https://doi.org/10.1088/1742-6596/2360/1/012030.
[16] C. long Guan, L. hua Zhan, D. chao Zhang, S. ming Yao, S. cong Zhong, B. Wang, Microwave uniformity regulation and its influence on temperature field distribution of composite materials, J. Cent. South. Univ. 30 (2023), https://doi.org/10.1007/s11771-023-5458-6.
[17] S.K. Satpathy, L.G. Tabil, V. Meda, S.N. Naik, R. Prasad, Torrefaction of wheat and barley straw after microwave heating, Fuel 124 (2014), https://doi.org/10.1016/j.fuel.2014.01.102.
[18] S.A. Halim, J. Swithenbank, Simulation study of parameters influencing microwave heating of biomass, J. Energy Institute 92 (2019), https://doi.org/10.1016/j.joei.2018.05.010.
[19] C. Song, T. Wu, Z. Li, J. Li, H. Chen, Analysis of the heat transfer characteristics of blackberries during microwave vacuum heating, J. Food Eng. 223 (2018), https://doi.org/10.1016/j.jfoodeng.2017.11.040.
[20] M.Y. Ong, S. Nomanbhay, Design and modelling of an enhanced microwave reactor for biodiesel production, Int. J. Scientif. Res. Public. (IJSRP) 8 (2018), https://doi.org/10.29322/ijsrp.8.12.2018.p8465.
[21] S.P. Yeong, M.C. Law, K.Y. You, Y.S. Chan, V.C.C. Lee, A coupled electromagnetic-thermal-fluid-kinetic model for microwave-assisted production of Palm Fatty Acid Distillate biodiesel, Appl. Energy 237 (2019) 457–475, https://doi.org/10.1016/j.apenergy.2019.01.052.
[22] S.P. Yeong, M.C. Law, C.C. Vincent Lee, Y.S. Chan, Modelling batch microwave heating of water, IOP. Conf. Ser. Mater. Sci. Eng. 217 (2017), https://doi.org/10.1088/1757-899X/217/1/012035.
[23] Z. Wang, Y. Hu, H. Lu, F. Yu, Dielectric properties and crystalline characteristics of borosilicate glasses, J. Non. Cryst. Solids. 354 (2008), https://doi.org/10.1016/j.jnoncrysol.2007.01.099.
[24] N.A.M. Aziz, Transesterification of Palm-Based Methyl Ester and Trimethylolpropane For Trimethylolpropane Esters Production Using Microwave-Assisted Heating, Universiti Putra Malaysia, 2021.
[25] J.R. White, Measuring the strength of the microwave field in a cavity, J. Microw. Power 5 (1970), https://doi.org/10.1080/00222739.1970.11688755.
[26] N.A.M. Aziz, H.A. Hamid, R. Yunus, Z. Abbas, R. Omar, U. Rashid, A.M. Syam, Kinetics and thermodynamics of synthesis of palm oil-based trimethylolpropane triester using microwave irradiation, J. Saudi Chem. Soc. 24 (2020), https://doi.org/10.1016/j.jscs.2020.05.006.
[27] H.A. Hamid, R. Yunus, U. Rashid, T.S.Y. Choong, S. Ali, A.M. Syam, Synthesis of high oleic palm oil-based trimethylolpropane esters in a vacuum operated pulsed loop reactor, Fuel 166 (2016) 560–566, https://doi.org/10.1016/j.fuel.2015.11.022.
[28] R. Yunus, A. Fakhru'l-Razi, T.L. Ooi, S.E. Iyuke, J.M. Perez, Lubrication properties of trimethylolpropane esters based on palm oil and palm kernel oils, Europ. J. Lipid Sci. Technol. 106 (2004) 52–60, https://doi.org/10.1002/ejlt.200300862.
[29] N. Haneishi, S. Tsubaki, E. Abe, M.M. Maitani, E. ichi Suzuki, S. Fujii, J. Fukushima, H. Takizawa, Y. Wada, Enhancement of fixed-bed flow reactions under microwave irradiation by local heating at the vicinal contact points of catalyst particles, Sci. Rep. 9 (2019) 1–12, https://doi.org/10.1038/s41598-018-35988-y.
[30] H. Nigar, G.S.J. Sturm, B. Garcia-Baños, F.L. Peñaranda-Foix, J.M. Catalá-Civera, R. Mallada, A. Stankiewicz, J. Santamaría, Numerical analysis of microwave heating cavity: combining electromagnetic energy, heat transfer and fluid dynamics for a NaY zeolite fixed-bed, Appl. Therm. Eng. 155 (2019) 226–238, https://doi.org/10.1016/j.applthermaleng.2019.03.117.
[31] P. Rattanadecho, The simulation of microwave heating of wood using a rectangular wave guide: influence of frequency and sample size, Chem. Eng. Sci. 61 (2006) 4798–4811, https://doi.org/10.1016/j.ces.2006.03.001.
[32] P. Rattanadecho, N. Suwannapum, W. Cha-um, interactions between electromagnetic and thermal fields in microwave heating of hardened type I-cement paste using a rectangular waveguide (influence of frequency and sample size), J. Heat. Transfer. 131 (2009) 1–12, https://doi.org/10.1115/1.2993134.
[33] K. Pitchai, J. Chen, S. Birla, R. Gonzalez, D. Jones, J. Subbiah, A microwave heat transfer model for a rotating multi-component meal in a domestic oven: development and validation, J. Food Eng. 128 (2014) 60–71, https://doi.org/10.1016/j.jfoodeng.2013.12.015.
[34] H. Li, S. Shi, B. Lin, J. Lu, Y. Lu, Q. Ye, Z. Wang, Y. Hong, X. Zhu, A fully coupled electromagnetic, heat transfer and multiphase porous media model for microwave heating of coal, Fuel Process. Technol. 189 (2019) 49–61, https://doi.org/10.1016/j.fuproc.2019.03.002.
[35] H. Prosetya, A. Datta, Batch microwave heating of liquids. An experimental study, J. Microw. Power Electromagn. Energy 26 (1991) 215–226, https://doi.org/10.1080/08327823.1991.11688160.
[36] S. Ryynänen, P.O. Risman, T. Ohlsson, Hamburger composition and microwave heating uniformity, J. Food Sci. 69 (2004) 187–196, https://doi.org/10.1111/j.1365-2621.2004.tb13619.x.
[37] P. Zhao, W. Gan, C. Feng, Z. Qu, J. Liu, Z. Wu, Y. Gong, B. Zeng, Multiphysics analysis for unusual heat convection in microwave heating liquid, AIP. Adv. 10 (2020) 1–7, https://doi.org/10.1063/5.0013295.
[38] R. Akarapu, B.Q. Li, Y. Huo, J. Tang, F. Liu, Integrated modelling of microwave food processing and comparison with experimental measurements, J. Microw. Power Electromagn. Energy 39 (2004) 153–165, https://doi.org/10.1080/08327823.2004.11688516.